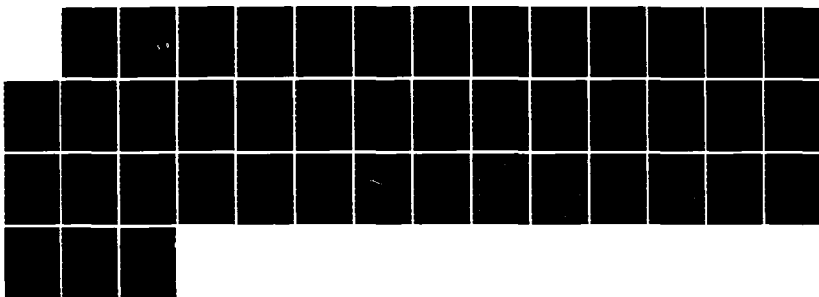
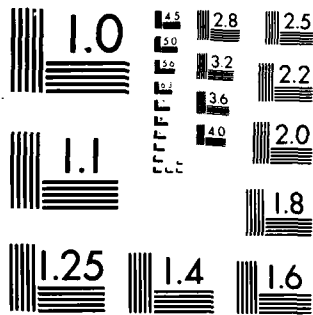


AD-A173 944

MONTE CARLO SIMULATION STUDIES OF THE POLYMERIZATION OF 1/1  
POLYURETHANE BLOC. (U) WISCONSIN UNIV-MADISON DEPT OF  
CHEMICAL ENGINEERING J A MILLER ET AL. 88 OCT 86 10  
N00014-83-K-0423 F/G 11/79 NL

UNCLASSIFIED





MICROCOPY RESOLUTION TEST CHART  
NATIONAL BUREAU OF STANDARDS-1963-A

## REPORT DOCUMENTATION PAGE

READ INSTRUCTIONS  
BEFORE COMPLETING FORM

12

1. REPORT NUMBER 10	2. GOVT ACCESSION NO.	3. RECIPIENT'S CATALOG NUMBER
4. TITLE (and Subtitle) Monte Carlo Simulation of Polymerization of Polyurethane Block Copolymers. 3. Modelling Premature Phase Separation during Reaction		5. TYPE OF REPORT & PERIOD COVERED
7. AUTHOR(s) J.A. Miller, T.A. Speckhard, I.G. Homan, and S.L. Cooper		6. PERFORMING ORG. REPORT NUMBER
8. PERFORMING ORGANIZATION NAME AND ADDRESS Chemical Engineering Department University of Wisconsin, Madison, WI 53706		9. CONTRACT OR GRANT NUMBER(s) N00014-83-K-0423
11. CONTROLLING OFFICE NAME AND ADDRESS Office of Naval Research 800 N. Quincy Street Arlington, VA 22217		10. PROGRAM ELEMENT, PROJECT, TASK AREA & WORK UNIT NUMBERS
14. MONITORING AGENCY NAME & ADDRESS (if different from Controlling Office)		12. REPORT DATE Oct. 8, 1986
15. SECURITY CLASS. (of this report) Unclassified		13. NUMBER OF PAGES
16. DISTRIBUTION STATEMENT (of this report) Approved for public release, distribution unlimited.		14. SECURITY CLASSIFICATION DOWNGRADING SCHEDULE

14. DISTRIBUTION STATEMENT (of this report)

Approved for public release, distribution unlimited.

17. DISTRIBUTION STATEMENT (of the abstract in this report) (If different from 14)

18. SUPPLEMENTARY NOTES

To be published in Polymer.

19. KEY WORDS (and Descriptors) (Enter on separate line)

Monte Carlo Simulation, Sinking Ring Model, Composition Distribution, Molecular Weight Distribution, Reactivities.

20. ABSTRACT (Enter on separate line)

See next page.

**SDIC**  
**ELECTE**  
NOV 04 1986  
**S D**  
**E**

DD FORM 1 JAN 73 1473

AD-A173 944

SDIC FILE COPY

ABSTRACT

Because of the complexities involved in polyurethane reaction chemistry and the difficulties encountered in making experimental measurements, relatively little attention has been paid to determining the precise molecular weight, composition, and hard segment length distributions of polyurethane block copolymers. ~~Yet,~~ the available evidence suggests that variations in these distributions can markedly influence structure-property relationships in these materials. ~~Therefore,~~ computer models have been developed using Monte Carlo methods that allow for simulation of the polymerization process under various conditions and subsequent calculation of the various distributions. The model developed in this contribution is based on a sinking pool of monomers and is thus termed the simple sinking pool model. This model offers several advantages over previous models; in particular it can simulate effects due to differing reactivity of the chain extender and the polyol, and effects due to phase separation occurring at varying points in the reaction. The model and rationale behind the inclusion of the various parameters are described, and the effects of varying the model parameters on the simulated composition, molecular weight, and hard segment length distributions are determined and discussed.

1



Accession For	
NTIS GRA&I	<input checked="" type="checkbox"/>
DTIC TAB	<input type="checkbox"/>
Unannounced	<input type="checkbox"/>
Justification	
By _____	
Distribution/	
Availability Codes	
Dist	Avail and/or Special
A-1	

*Studies*  
Monte Carlo Simulation ~~Study~~ of the Polymerization of Polyurethane  
Block Copolymers. III. Modelling of Premature Phase Separation  
During Reaction and Differing Reactivities  
of the Chain Extender and Polyol Using the Simple Sinking Pool Model

John A. Miller\*  
Thomas A. Speckhard\*  
James G. Homan  
Stuart L. Cooper\*\*

Department of Chemical Engineering  
University of Wisconsin  
Madison, Wisconsin 53706

January, 1986

Revised May 1986

\* Current Address: 3M Research Center, St. Paul, MN 55144  
\*\* Author to whom correspondence should be addressed.

UW Code: 110A-SLC

86 11 3 007

### ABSTRACT

Because of the complexities involved in polyurethane reaction chemistry and the difficulties encountered in making experimental measurements, relatively little attention has been paid to determining the precise molecular weight, composition, and hard segment length distributions of polyurethane block copolymers. Yet, the available evidence suggests that variations in these distributions can markedly influence structure-property relationships in these materials. Therefore, computer models have been developed using Monte Carlo methods that allow for simulation of the polymerization process under various conditions and subsequent calculation of the various distributions. The model developed in this contribution is based on a sinking pool of monomers and is thus termed the simple sinking pool model. This model offers several advantages over previous models; in particular it can simulate effects due to differing reactivity of the chain extender and the polyol, and effects due to phase separation occurring at varying points in the reaction. The model and rationale behind the inclusion of the various parameters are described, and the effects of varying the model parameters on the simulated composition, molecular weight, and hard segment length distributions are determined and discussed.

## I. Introduction

Polyurethane block copolymers can be polymerized under a wide variety of conditions leading to different molecular weight, hard segment length and composition distributions<sup>1-5</sup>. The effects of changing these distributions on sample properties and morphology are not well understood because of the difficulties in obtaining accurate experimental characterization of the distributions<sup>6-8</sup> and because the complexity of the polyurethane reaction has hindered the development of a direct theoretical approach for calculating the various distributions under given polymerization conditions. Peebles<sup>4,5</sup> has shown that under certain ideal conditions the hard segment length distribution should follow a most probable distribution. In the first contribution of this series<sup>1</sup>, Peebles' ideal conditions and the assumption of a most probable distributor for the degree of polymerization in terms of hard and soft segments were used as the basis for a Monte Carlo simulation method that calculated the corresponding composition and molecular weight distributions. In the second contribution of this series<sup>2</sup>, the original model was modified to simulate premature phase separation during polymerization. Premature phase separation has been observed at the beginning of or at later points in bulk reactions by several investigators<sup>9-14</sup>. Depending on the particular system the source of the phenomena has been attributed to the incompatibility of the reactant monomers, incompatibility of the polymer and monomer, and crystallization of the polymer. In the modified model the reactants were partitioned into two phases at the start of the reaction and thus the model is best suited for the simulation of phase separation due to monomer incompatibility occurring immediately at the beginning of the reaction. The model showed how premature phase separation can lead to broader hard segment length and molecular weight distributions and

"excess" compositional heterogeneity.

Both of the above models, the so-called single-phase and two-phase ideal reaction models, are termed ideal because they utilize the simplifying assumptions proposed by Peebles<sup>4,5</sup>. Several of the assumptions, in particular the equal reactivity of the chain extender and polyol hydroxyl groups and the equal reactivity of all isocyanate and hydroxyl groups regardless of the molecular weight of the growing chain, are likely to be poor approximations of actual behavior under normal conditions especially in bulk polymerizations. Eisenbach<sup>15</sup> has recently shown that the distribution of products from the first step of a two-step bulk reaction does not follow the distribution predicted by Peebles. Therefore, the actual hard segment length distribution will differ from that calculated using Peebles' approach. Although the hard segment length, molecular weight, and composition distributions calculated using the single-phase and two-phase ideal reaction models are useful for comparison purposes, it is clear that these models have several shortcomings for simulating the actual polymerization behavior of polyurethane block copolymers. Therefore, in this contribution a different method, again based on a Monte Carlo simulation, is developed and described. This model based on a sinking pool of monomers is termed the simple sinking pool model and is described in the next section. The effects of varying the model parameters on the calculated hard segment length, composition, and molecular weight distribution are then described. The ability of all three models to simulate actual experimental data of MacKnight and coworkers on polybutadiene polyurethanes<sup>9,10</sup> will be evaluated and compared in another contribution<sup>16</sup>.

## II. Model Description

The model described in this contribution, termed the simple sinking pool model, has three major improvements over the previous models. The first

improvement is to allow for different effective reactivities for the chain extender and the polyol. The intrinsic rate constant<sup>17</sup> for each species reacting with an isocyanate group may be the same, but the effects of viscosity and diffusion may make the effective rate constants, especially in bulk reactions, different. These effects are accounted for. The second advance allows for the simulation of phase separation occurring at various points and not just at the beginning of the reaction.

The third improvement over the previous models is in the use of a sinking pool of monomers for the Monte Carlo modelling. In the first two models, the chains were built up sequentially by whole segments from an infinite pool of segments. In this simulation the pool of monomers is finite; therefore, the simulation more accurately reflects the actual polymerization conditions. The probability of a given species being the next to react is not constant as in the first models, but depends on the number of that type of monomer remaining in the pool.

The various parameters used in the model, several of which are used to effect the improvements noted above, are described below.

- Reaction Stoichiometry -- Molar ratios of diisocyanate/chain extender/  
polyol. The reaction need not be stoichiometric.
- Types of Monomers----- A number of different typical reactants can be used.
- Soft Segment Molecular
- Weight Distribution----- The polyol average molecular weight and distribution  
can be specified.
- $\bar{D}_p$  ----- The average degree of polymerization in terms  
of monomer units.
- RCF ----- The reaction competitiveness factor, which is  
defined as the effective reactivity of the

chain extender divided by the effective reactivity of the polyol. This quantity takes into account the differences in the intrinsic rate constants and the differences in the diffusivities of the chain extender and polyol.

SAF ----- The self-affinity factor, a parameter that is used to describe premature phase separation during the polymerization. Higher values of SAF correspond to greater incompatibility of the reactants and therefore a greater propensity for phase separation.

NSA ----- Degree of polymerization at which the effect of self-affinity begins. It has been noted by a number of workers<sup>11-14</sup> that phase separation often does not occur until a certain hard segment length has been achieved. This parameter is used to describe this or similar situations.

Upper and Lower  $D_p$  ----- Because of limitations on the computer, an upper limit for the degree of polymerization must be set. Practically this has little effect. The lower limit on the degree of polymerization can be used to model the effect of a precipitation step for a solution polymerization where the low molecular weight species are often lost.

Number of Chains----- The number of polymer chains to build up,  
typically 15,000.

Once the values for the above parameters are chosen, the model is then implemented in the following manner.

The first step is to set up three separate pools of monomers, one for each type, based on the stoichiometry, the average degree of polymerization, and the total number of chains. A large array is then established where each row corresponds to one chain and each column to a monomer position. Within each row there will be a section of empty cells, a section of contiguous monomers that form the chain, then a final section of empty cells, so not all cells in the array will be filled with monomers at the end of the simulation process. The point within the row that the chain begins (the start of the polymerization process) is chosen at random so that the effect of depleting a monomer pool is not felt only by the chains with a large degree of polymerization. The degree of polymerization for each chain is also chosen at random such that the overall distribution of the degree of polymerization follows the most probable distribution and that the average value corresponds to that selected initially. The simulation proceeds in a step-wise parallel fashion, starting with the first column and continuing row by row. At the end of the column, the process continues on the subsequent column until the entire array has been operated on.

To visualize the simulation process, consider the cell in the array at (N,M), which corresponds to the Nth chain and the Mth position along the Nth row. We must first determine if the chain is growing at this point. If M is smaller than the point at which the chain begins or greater than the starting point plus the degree of polymerization of the Nth chain, nothing happens and we move on to the next cell. If not, the chain is growing and

we must next determine what type of monomer is to be placed in this cell. If the previous cell (N,M-1) contains a chain extender or a polyol, then this cell must receive a diisocyanate. If (N,M-1) contains a diisocyanate, then a choice must be made between placing a chain extender in (N,M) or placing a polyol in (N,M). This choice is the key point in the simulation procedure.

The next step is to calculate the probability of adding a chain extender next (vs. polyol) based on several factors including the number of monomers of each type left in the pool (concentration), the reaction competitiveness factor, and self-affinity effects. Of these, the self-affinity effect requires the most calculation. If the current degree of polymerization of chain N is less than the value of the onset of self-affinity (NSA), we proceed directly to the calculation of the probability of reacting with a chain extender. Otherwise we look at the last five diol (chain extender (C) or polyol (P)) species that have been added to the chain. The most recent diol is assigned a value of 2.0, the second most recent a 1.7, and the remainder 1.4, 1.2 and 1.0. These values are then summed for chain extender species and for polyols and 1.0 is added to each sum. These sums are then multiplied by the self-affinity factor (SAF). The basic concept behind this process is that a chain that has recently been adding primarily chain extenders is likely to be in a hard segment rich (chain extender rich) phase and is thus more likely to continue to add chain extenders. The reverse situation applies for chains that have recently been adding polyol. Thus if the last five diols in the chain are CCCCCP and SAF is unity, the total self-affinity sum for the polyol would be 2.0, while for the chain extender it would be 7.3. These sums are then used in the calculation of the probability of reacting with a chain extender. (These sums are 1.0 when the chain  $D_p$  is less than NSA.) The probability of

reacting with a chain extender is then given by

$$P_C = \frac{N_C * SA_C * RCF}{N_C * SA_C * RCF + N_P * SA_P}$$

where  $N_C$  and  $N_P$  are the number of chain extenders and polyols left in the pools,  $SA_C$  and  $SA_P$  are the sums for the self-affinity contributions, and RCF is the reaction competitiveness factor. Based on this probability, either a polyol or a chain extender is placed in cell (N,M). The appropriate monomer pool is then depleted by one unit and this whole process is repeated for cell (N+1,M).

After all of the cells in the array have been processed in the above fashion, the chain statistics are calculated. The polyol molecular weight is selected at random so that it conforms to the appropriate average and distribution. The hard segment length, molecular weight and composition distributions are the main parameters that are tabulated during this step.

The second part of the modelling procedure for the simple sinking pool model involves a simulation of a solvent fractionation of a sample. Although as noted in the first contribution of this series<sup>1</sup>, the fractionation process probably depends on both the molecular weight and composition, in this step it is assumed that fractionation occurs only on the basis of composition. To simulate a fractionation where the soft segment-rich fraction comprises 30% of the total weight of the polymer chains, the model starts with the chains with the lowest hard segment content and sums their weight fraction until a value of 0.3 is reached. The average composition,  $\bar{M}_n$  and  $\bar{M}_w$  of this fraction is then calculated. Similar quantities are also calculated for the remaining hard segment-rich fraction. The model can also calculate several fractionation points concurrently; these fractions are all calculated starting with the lowest hard segment content species.

The simple sinking pool model is primarily intended for studying the premature phase separation phenomenon in a one-step bulk polymerization. However, the model can also be extended to other polymerization conditions. A one-step homogeneous solution polymerization can be modelled using the simple sinking pool model since it allows for differing rates of reaction of the polyol and the chain extender.

As currently implemented the model has several shortcomings. The model does not allow for unequal reactivity of the isocyanate groups on the diisocyanate which will introduce some error in modelling a two-step reaction. The model assumes a most probable distribution, MPD, for the  $D_p$  distribution under conditions that should produce deviations from the MPD. It should be noted that there is presently no direct method for calculating what the  $D_p$  distribution should be under conditions where the reactivity of monomers varies throughout the reaction. It should be possible to calculate the  $D_p$  distribution under these conditions using an approach similar to Chaumont et al.<sup>18</sup> where the  $D_p$  of a chain is not predetermined and chains do not react only with monomers. Instead all species in the pool (i.e. dimers, trimers, etc.) can react with all other species. The model also ignores the effect of molecular weight on reactivity, and the modelling of phase separation by the self-affinity concept does not allow for different reaction rates in the two phases. Finally, the model allows for non-stoichiometric reaction conditions but does not include crosslinking effects. By combining and modifying the simple sinking pool method with some of the concepts and methods of the other approaches discussed previously<sup>1,2,18</sup> it is hoped that more realistic models can be developed. At this point the model is not intended to be an absolutely accurate description of polyurethane polymerizations but it can

be utilized to achieve a qualitative understanding of the effects of various polymerization conditions on the resulting molecular weight, hard segment length, and composition distributions.

### III. Results and Discussion

For comparison purposes a reference or base case is defined with the following characteristics and parameter values. The standard stoichiometry is defined as a 3/2/1 mole ratio of methylene bis(p-phenyl isocyanate)(MDI), butanediol (BD), and poly(tetramethylene oxide) (PTMO). The soft segment has a number-average molecular weight of 1008 and a weight-average molecular weight of 1450, with a molecular weight distribution described by the HPLC data reported by Miller et al.<sup>19</sup> The average degree of polymerization for the base case is 100, the RCF is 1, and no self-affinity is used. The lower bound for the degree of polymerization is 1 monomer unit and the upper bound is 1500. The number of chains used for the Monte Carlo simulation was fixed at 15000.

The reference parameters (base case) for the sinking pool model produced the following molecular weight hard segment length and composition characteristics. The number-average molecular weight was 31850, the value of  $\bar{M}_w/\bar{M}_n$  was 1.93, the hard segment number-average length (number of isocyanate units ( $\bar{K}_n$ )) was 2.88, and the hard segment  $\bar{K}_w/\bar{K}_n$  was 1.65 ( $\bar{K}_w$  is weighted by the number of isocyanate units). The hard segment fraction of the 10 weight-percent soft segment-rich fraction was 0.372 and the 50 weight-percent soft segment-rich fraction had a hard segment fraction of 0.432. The total sample had a hard segment weight fraction of 0.481. These values are similar to the base case values for the single-phase ideal reaction model<sup>1</sup> ( $\bar{M}_n = 28520$ ,  $\bar{M}_w/\bar{M}_n = 1.96$ , 0.369 and 0.430 hard segment weight fractions for the 10 and 50 weight-percent soft segment-rich fractions, and an overall hard segment content of 48.1%). This agreement is not surprising since both cases have the same stoichiometry and soft segment

characteristics and do not include non-ideal effects. The differences between the models are due to the differences in the  $\bar{D}_p$  values and how the degree of polymerization is defined as well as the use of a diisocyanate reactivity ratio ( $\mu$ ) of 3 to calculate the hard segment distribution in the single-phase ideal reaction model. The net effect of these differences has been partially compensated for by choosing the base case  $\bar{D}_p$  value for the simple sinking pool model so that slightly higher molecular weight values, which lead to less compositional heterogeneity, are produced. The agreement between the two sets of base case values also indicates that the error involved in using a block degree of polymerization instead of a  $D_p$  based on monomers in the single-phase ideal reaction model does not significantly affect the composition and molecular weight distributions at the base value of the block degree of polymerization.

Varying the parameters common to both the single phase ideal reaction model and the simple sinking pool model such as the degree of polymerization, reaction stoichiometry, soft segment molecular weight and molecular weight distribution, and the limit of the lower degree of polymerization leads to similar trends in the composition, hard segment length and molecular weight distributions for the same reasons noted previously for the single-phase ideal reaction model<sup>1</sup>. Therefore, the discussion of results for these parameters will be limited to the effects of varying  $\bar{D}_p$  and will include the effects on the hard segment distribution which was fixed for a given stoichiometry and  $\mu$  value in the single-phase reaction model.

Table 1 shows that increasing the value of  $D_p$  leads to an increase in the molecular weight and a decrease in the compositional heterogeneity as expected. The compositional heterogeneity can be estimated using the fractional composition values for the 0.1 and 0.5 soft segment-rich weight fractions. The more compositionally homogenous the material, the closer the values for the hard

segment content of the soft segment-rich fraction should approach the average hard segment content of the sample. The effect of increasing  $\bar{D}_p$  on the compositional heterogeneity can also be seen in Figure 1.

The abscissa in Figure 1 is the cumulative weight fraction of chains in ascending order of hard segment composition. As the  $x$  value increases, the chains within an  $x$  interval possess a higher average hard segment content than chains in previous  $x$  intervals. The ordinate is a measure of this change and is the fraction of hard segment material in the chains within the specific  $x$  interval. This quantity is called the specific hard segment weight fraction. Since a compositionally homogeneous sample would exhibit a horizontal line at the average composition value, these data clearly indicate the decrease in compositional heterogeneity with increasing  $\bar{D}_p$ . When comparing the data in the tables and figures it should be remembered that the fractional compositions in the tables are cumulative average values up to a certain cumulative weight fraction, whereas the figures are specific compositions at certain cumulative weight fraction intervals.

The effect of increasing  $\bar{D}_p$  on the hard segment distribution can be observed by examining the  $\bar{R}_n$  and  $\bar{R}_w/\bar{R}_n$  values in Table 1 (number average and ratio of weight to number average hard segment length in terms of isocyanate units). As  $\bar{D}_p$  approaches  $\infty$  (conversion goes to 100%) Peebles<sup>4,5</sup> showed that for an 3/2/1 stoichiometry under ideal conditions the values of  $\bar{R}_n$  and  $\bar{R}_w/\bar{R}_n$  should approach 3.0 and 1.66, respectively. The data in Table 1 exhibits the expected behavior but it is interesting to note the large deviation at low  $\bar{D}_p$  from the 100% conversion values, especially for  $\bar{R}_n$ .

The data in Table 1 also indicate that the  $\bar{M}_w/\bar{M}_n$  values which normally would be expected to increase with  $\bar{D}_p$  actually decrease. The  $\bar{N}_w/\bar{N}_n$  values which are the ratio of the weight and number average degrees of polymerization do

increase and exhibit the values predicted by Flory<sup>17</sup>. This anomalous behavior has been observed and explained previously<sup>1</sup> and is due to the fact that the monomers do not all have the same molecular weight and the fact that a finite array is used to represent the  $D_p$  distribution.

Table 2 shows the effect of having a nonstoichiometric reaction (which was not allowed in the previous models) on the various distributions. Part A of the table uses a degree of polymerization that is the maximum for a given stoichiometry while Part B of the table holds the degree of polymerization constant as the stoichiometry is changed. The effect of changing the stoichiometry is very small, except in cases (Part A) where the stoichiometry will limit the average degree of polymerization significantly, in which case the influence of changes in  $\bar{D}_p$  will dictate the behavior of the molecular weight and distribution and the compositional heterogeneity. For typical bulk polymerization processes, where only a few percent excess diisocyanate is used, the influence of the nonstoichiometric conditions will be minimal. The above discussion, of course, neglects any effect due to crosslinking, which is likely to occur in systems with excess isocyanate.

To this point only reaction conditions which affect the natural heterogeneity of a system have been discussed. The first factor that leads to excess compositional heterogeneity is the unequal effective reactivities of the polyol and the chain extender. Table 3 shows the effect of changing the RCF for the 3/2/1 MDI/BD/PTMO system. The number average molecular weight of the polymer is unaffected by RCF, as expected. However, as the RCF deviates from a value of 1, the breadth of the molecular weight distribution as measured by  $\bar{M}_w/\bar{M}_n$  increases substantially. The effect on  $\bar{M}_w/\bar{M}_n$  is greater for variations in RCF than for any of the factors which only affect the natural compositional heterogeneity. A similar situation exists for the hard segment length distribution. The average

length ( $\bar{K}_n$ ) does not change appreciably with changes in the reaction competitiveness factor, but as the RCF deviates from 1, the value of  $\bar{K}_w/\bar{K}_n$  increases. For the compositional heterogeneity, again the same situation exists in that as the RCF deviates from unity, the difference between the average and fractional composition increases. The increase in compositional heterogeneity can be seen in Figures 2a to 2c, which show three-dimensional histograms of composition and molecular weight on the x-axis and y-axis while the z-axis represents the relative number of chains with compositions and molecular weight values corresponding to that section of the grid. As the RCF increases from 0.1 to 1.0, the molecular weight-composition data shift toward a more homogeneous system. As the RCF increases further, the system becomes more heterogeneous.

The effect of varying RCF on the composition distribution can also be seen in Figure 3. For RCF = 1 the composition curve exhibits a shape typical of an ideal system with some natural heterogeneity<sup>1</sup>. When RCF = 0.1 the system becomes much more heterogeneous and the composition curve is no longer symmetric, indicating the presence of non-ideal effects. In particular, there is a large weight fraction of material that is almost pure hard segment. This is because when RCF = 0.1, most of the polyol reacts early in the reaction, depleting the pool of polyol, and thus chains reacting towards the end of the polymerization are almost entirely isocyanate and chain extender. The opposite situation occurs when RCF = 10.0, but since there is always some isocyanate in a chain (unless  $D_p = 1$ ) there is little pure soft segment material. Note however, that the average hard segment content of the most soft segment-rich material does decrease. Finally, it is obvious that the fractional composition data presented in Table 3 do not necessarily indicate which sample is more compositionally heterogeneous when non-ideal effects are being considered because

the composition curves are no longer symmetric. For example, the data in Table 3 would indicate that an RCF of 10 leads to greater compositional heterogeneity than an RCF of 0.1, but, as noted previously<sup>2</sup>, this is because these data are sensitive to the fraction of material that is very rich in soft segments, corresponding to the left-hand portion of Figure 3.

The effect of RCF on the hard segment length distribution can be seen in Figures 4a to 4c. A histogram of weight fraction (number fraction weighted by the length of the hard segment) versus length of the hard segment (number of diisocyanate units) is shown in Figure 4a for an RCF = 1.0, which results in a most probable distribution (MPD) as indicated by Peebles<sup>4,5</sup>. (There is a slight deviation from an MPD because the conversion is not 100%.) Figures 4b and 4c show the distribution for values of RCF = 0.1 and 10, respectively. In both cases there are more longer and more shorter hard segments than is the case for the MPD. Comparing the data in Figures 4b and 4c indicates that fewer single unit hard segments are produced when RCF = 0.1 than when RCF = 10. When RCF = 10 the chain extender pool becomes depleted during the reaction and thus the remaining hard segments must be one diisocyanate unit long. When RCF = 0.1 it is favorable to form hard segments that are only one unit long early in the reaction, but there is always a finite chance of forming longer hard segments. Thus, fewer one unit long hard segments but more 2 unit long hard segments are formed when RCF = 0.1 as compared with RCF = 10.0. The situation is reversed for long hard segments. Although the data shown in Figures 4b and 4c do not extend out to high enough hard segment lengths for the effect to be observed, the case with RCF = 0.1 actually has more very long hard segments than the case with RCF = 10 (weight fractions are less than 0.0003 for hard segment lengths greater than 66 when RCF = 10.0 but not until hard segment lengths are greater

than 148 for RCF = 0.1). The large effect on  $\bar{K}_w$  due to very long hard segments is reflected in the larger  $\bar{K}_w/\bar{K}_n$  values for RCF = 0.1 compared with RCF = 10.0 in Table 3.

The other factor which can cause excess compositional heterogeneity is the self-affinity factor SAF which is used to model phase separation. Table 4a shows the effect of changing the self-affinity factor on the molecular weight and distribution, the hard segment molecular weight distribution, and the compositional heterogeneity. The stoichiometry for these simulations was 3/2/1, the degree of polymerization was 100, and the RCF was unity. Additionally, the  $D_p$  value for a given chain at which self-affinity effects begin (NSA) was fixed at 10.  $\bar{M}_n$  and  $\bar{K}_n$  are unaffected by the changes in the SAF as expected. As the SAF increases, the molecular weight distribution of the whole polymer becomes broader as does the hard segment length distribution. The data in Table 4a and in Figure 5 show that the compositional heterogeneity also increases significantly as the SAF is increased. Figures 6a and 6b show three-dimensional histograms for the cases where the self-affinity factor is 1 and 10 respectively. The three-dimensional histogram for the case where the SAF is zero was shown in Figure 2b. The central ridge in Figure 2b spreads out in Figure 6a and spreads even further in Figure 6b, indicative of a broadening of the distribution of compositions at all molecular weights as the SAF is increased. These effects are not surprising, since as the SAF rises, the tendency for chains to propagate with the same type of segment increases, leading to broader hard segment length, composition and molecular weight distributions.

Part B of Table 4 shows the effect of varying the  $D_p$  value at which self-affinity effects begin (NSA) in an individual chain at a constant SAF value. Varying the NSA value can be done to effectively simulate phase separation

occurring at different points in a reaction. As NSA increases phase separation would effectively occur later and its influence on molecular characteristics would be diminished. Thus as NSA increases, effects due to self-affinity decrease as evidenced by the data in Table 4b. Note in particular the large decrease in  $\bar{K}_w/\bar{K}_n$  values as NSA increases.

The results from Tables 3 and 4 indicate that the effects on the various distributions of the RCF and SAF are quite similar. This is not surprising since each factor effectively functions by depleting one of the monomer pools. Thus, if one were to evaluate actual experimental data it would be practically impossible without additional information (e.g. phase separation did not occur) to distinguish between effects due to unequal reactivity or phase separation. However, the physical basis for these effects are independent and with a different type of model, for example where phase separation is modelled by partitioning, it should be possible to separate the effects.

Table 5 shows the behavior of systems where both the self-affinity factor (SAF) and the reaction competitiveness factor (RCF) are varied. As expected, these two effects can influence each other markedly since each mechanism attempts to deplete one of the monomer pools and thus competes for effect. At larger SAF values, changes in RCF produce smaller changes in the whole chain and hard segment molecular weight distributions and the compositional heterogeneity. Similarly, as the RCF deviates from unity, the effect of changes in the SAF on the various distributions is diminished. Nevertheless, when RCF deviates from 1 and SAF is greater than zero, very broad hard segment length and composition distributions can be obtained as indicated by the data in Table 5 and Figure 7. Note that the composition distribution in Figure 7 is what one would expect from a blend of two materials with a large difference in hard segment contents and is

similar to those obtained using the two-phase ideal reaction model<sup>2</sup>.

Table 6 shows the effect of varying the degree of polymerization under various non-ideal conditions (the effects of varying  $\bar{D}_p$  under ideal conditions [RCF = 1, SAF = 0] were shown in Table 1 and Figure 1). The same trends noted in Table 1 are observed; as  $\bar{D}_p$  increases,  $\bar{M}_w/\bar{M}_n$  and the compositional heterogeneity decrease, while  $\bar{K}_w/\bar{K}_n$  increases. What is somewhat surprising are the large changes in  $\bar{K}_w/\bar{K}_n$  as  $\bar{D}_p$  is varied. The large variability in  $\bar{K}_w/\bar{K}_n$  is due to the fact that at higher  $\bar{D}_p$  values there are more monomers in the pool thereby allowing for greater depletion effects, and because the effect of limited chain length restricting hard segments lengths is reduced. Thus, increasing  $\bar{D}_p$  tends to accentuate the effects of varying SAF and RCF on the hard segment length distribution but reduces the effect on the composition and molecular weight distributions.

Finally, it should be noted that while the effects of varying SAF and NSA (and also RCF) can produce results for the various distributions similar to those obtained using the two-phase ideal reaction model<sup>2</sup>, there are distinct differences between the models particularly in obtainable molecular weight distributions. These differences become apparent when the various models are used to simulate experimental data and will be discussed in another contribution<sup>16</sup>.

#### IV. Summary

An alternative Monte Carlo method has been developed and described that involves the use of a sinking pool of monomers and allows for calculation of the molecular weight hard segment length and composition distributions of polyurethane block copolymers under various polymerization conditions. This model offers several advantages over previous approaches including the ability to model different reactivities of the chain extender and polyol and

phase separation at various points in the reaction. Varying parameters such as the degree of polymerization, soft segment molecular weight distribution, and hard segment content that only affect the natural heterogeneity produced effects on the molecular weight and composition distributions similar to those described previously<sup>1</sup>. The effects of varying the reaction competitiveness factor (RCF), which was used to simulate differing reactivities of chain extender and polyol, and the self-affinity factor (SAF), which was used to model phase separation, were similar. Increasing SAF values or increasing the deviation of RCF from 1 led to a much broader hard segment length distribution, increased compositional heterogeneity, and a broader molecular weight distribution. The effects of varying SAF were also influenced by the choice of the degree of polymerization at which self-affinity effects begin (NSA). Higher NSA values correspond to phase separation occurring later in the reaction and resulted in a reduced influence of self-affinity on the various distributions. When both SAF and RCF deviate from ideal conditions the total effect will be less than the sum of the two individual effects since each mechanism can serve to deplete one of the monomer pools, and thus the two effects are competitive.

#### Acknowledgement

The authors would like to acknowledge partial support of this research by the National Science Foundation, Division of Materials Science, Polymer Section, Grant No. DMR 86-03839 and through a grant from the Office of Naval Research.

## References

1. T.A. Speckhard, J.A. Miller, and S.L. Cooper, *Macromolecules*, in press.
2. J.A. Miller, T.A. Speckhard, and S.L. Cooper, *Macromolecules*, in press.
3. J.H. Saunders and K.C. Frisch, *Polyurethane Chemistry and Technology: Part I. Chemistry*, Interscience, New York, 1962.
4. L.H. Peebles, *Macromolecules*, 7, 1872 (1974).
5. L.H. Peebles, *Macromolecules*, 9, 58 (1976).
6. D.C. Lee, T.A. Speckhard, A.D. Sorenson, and S.L. Cooper, *Macromolecules*, submitted for publication.
7. T.A. Speckhard and S.L. Cooper, *Rubber Chem. Tech.*, accepted for publication.
8. T.A. Speckhard, Ph.D. Thesis, University of Wisconsin-Madison (1985).
9. M. Xu, W.J. MacKnight, C.H.Y. Chen, and E.L. Thomas, *Polymer*, 24, 1327 (1983).
10. C.H.Y. Chen, R.M. Briber, E.L. Thomas, M. Xu, and W.J. MacKnight, *Polymer*, 24, 1333 (1983).
11. J.M. Castro, F. Lopez-Serrano, R.E. Camargo, C.W. Macosko, and M. Tirrell, *J. Appl. Polym. Sci.*, 26, 2067 (1981).
12. J.M. Castro, C.W. Macosko, and S.J. Perry, *Polym. Comm.*, 25, 83 (1984).
13. S.L. Hager, T.B. MacKury, R.M. Gerkin, and R.F. Critchfield, *A.C.S. Adv. Chem. Ser.*, 172, (1981).
14. R.E. Camargo, Ph.D. Thesis, University of Minnesota (1983).
15. C.D. Eisenbach, *A.C.S. Polymer Preprints*, 26(2), 7 (1985).
16. T.A. Speckhard, J.G. Homan, J.A. Miller, and S.L. Cooper, *Polymer*, submitted for publication.
17. P.J. Flory, *Principles of Polymer Chemistry*, Cornell University Press, Ithaca, NY, 1953.
18. P. Chaumont, Y. Gnanou, G. Hild, and P. Rempp, *Makromol. Chem.*, 186, 2321 (1985).
19. J.A. Miller and S.L. Cooper, *Makromol. Chem.*, 185, 2429 (1984).

TABLE 1

Effect of Varying the Degree of Polymerization on the Molecular Weight, Hard Segment Length, and Composition Distributions

3/2/1 MDI/BD/PTMO-1000(H), RCF=1.0, No Self-Affinity

$\bar{D}_p$	$\bar{M}_n$	$\bar{M}_w/\bar{M}_n$	$\bar{N}_w/\bar{N}_n$	Fractional Composition		Average Composition	$\bar{K}_n$	$\bar{K}_w/\bar{K}_n$
				0.1	0.5			
5	1592	2.099	1.800	0.110	0.270	0.484	1.67	1.48
10	3224	2.038	1.900	0.197	0.333	0.483	2.14	1.57
50	15750	1.968	1.980	0.331	0.413	0.481	2.78	1.64
100	31850	1.934	1.990	0.372	0.433	0.481	2.88	1.65
300	91020	1.880	1.886	0.414	0.452	0.481	2.96	1.66

TABLE 2

Effect of Having Nonstoichiometric Reaction Conditions  
on the Molecular Weight, Hard Segment Length  
and Composition Distributions

A/2/1 MDI/BD/PTMO-1000(H), RCF=1.0, No Self-Affinity

Moles of MDI (A)	$\bar{D}_p$	$\bar{M}_n$	$\bar{M}_w/\bar{M}_n$	Average Composition	Fractional Composition		$\bar{K}_n$	$\bar{K}_w/\bar{K}_n$
					0.1	0.5		
A. Degree of Polymerization Is Maximum for Stoichiometry								
3.05	120	37640	1.930	0.483	0.385	0.439	2.90	1.65
3.10	60	18930	1.964	0.487	0.352	0.425	2.81	1.64
3.20	30	9512	1.999	0.494	0.316	0.406	2.66	1.61
3.30	20	6306	2.003	0.499	0.287	0.390	2.52	1.59
3.50	12	3778	2.038	0.513	0.255	0.372	2.30	1.55
B. $\bar{D}_p$ Fixed at 30								
3.00	30	9570	1.963	0.481	0.292	0.394	2.64	1.62
3.05	30	9518	1.983	0.484	0.302	0.398	2.65	1.63
3.10	30	9557	1.979	0.488	0.306	0.401	2.65	1.62
3.20	30	9512	1.999	0.494	0.316	0.406	2.66	1.61

TABLE 3

Effect of Varying the Reaction Competitiveness  
Factor (RCF) on the Molecular Weight, Hard  
Segment Length and Composition Distributions

3/2/1 MDI/BD/PTMO-1000(H),  $\bar{D}_p=100$ , No Self-Affinity

<u>RCF</u>	<u><math>\bar{M}_n</math></u>	<u><math>\bar{M}_w/\bar{M}_n</math></u>	<u>Average Composition</u>	<u>Fractional Composition</u>		<u><math>\bar{K}_n</math></u>	<u><math>\bar{K}_w/\bar{K}_n</math></u>
				<u>0.1</u>	<u>0.5</u>		
0.1	31730	2.309	0.481	0.223	0.266	2.86	11.6
0.2	31730	2.189	0.481	0.257	0.308	2.87	6.86
0.5	31730	2.034	0.481	0.326	0.385	2.87	2.28
1.0	31850	1.934	0.481	0.372	0.433	2.88	1.65
2.0	31380	1.946	0.481	0.259	0.379	2.90	1.91
5.0	31650	2.134	0.481	0.192	0.282	2.91	2.96
10.0	31650	2.281	0.481	0.185	0.237	2.91	4.43

TABLE 4

Effect of Varying the Self-Affinity Factor (SAF)  
and the  $D_p$  at which Self-Affinity Effects Begin (NSA)  
on the Molecular Weight, Hard Segment Length  
and Composition Distributions

3/2/1 MDI/BD/PTMO-1000(H),  $\bar{D}_p=100$ , RCF=1.0

<u>SAF</u>	<u>NSA</u>	<u><math>\bar{M}_n</math></u>	<u><math>\bar{M}_w/\bar{M}_n</math></u>	<u>Average Composition</u>	<u>Fractional Composition</u>		<u><math>\bar{K}_n</math></u>	<u><math>\bar{K}_w/\bar{K}_n</math></u>
					<u>0.1</u>	<u>0.5</u>		
A. Constant NSA								
0	-	31850	1.934	0.481	0.372	0.433	2.88	1.65
.1	10	31240	1.903	0.480	0.347	0.421	2.88	1.89
.5	10	31640	1.946	0.480	0.289	0.382	2.89	2.90
1.0	10	31380	1.992	0.480	0.252	0.353	2.89	4.06
2.0	10	31430	2.023	0.481	0.224	0.322	2.89	5.97
5.0	10	31720	2.124	0.481	0.201	0.276	2.89	10.1
10	10	31710	2.211	0.481	0.195	0.244	2.89	13.4
100	10	31630	2.477	0.481	0.188	0.207	2.89	19.8
B. Constant SAF								
10	1	31810	2.020	0.480	0.183	0.237	2.89	15.2
10	3	31920	2.162	0.480	0.185	0.236	2.89	14.5
10	5	31240	2.208	0.480	0.187	0.236	2.89	13.6
10	10	31710	2.211	0.481	0.195	0.244	2.89	13.4
10	50	31730	2.015	0.480	0.226	0.306	2.89	10.0
10	100	31000	1.868	0.480	0.265	0.360	2.89	6.84

TABLE 5

Effect of Varying the Reaction Competitiveness Factor (RCF) on the Influence of the Self-Affinity Factor (SAF) on the Molecular Weight, Hard Segment Length and Composition Distributions

3/2/1 MDI/BD/PTMO-1000(H),  $\bar{D}_p=100$

<u>RCF</u>	<u>SAF</u>	<u><math>\bar{M}_n</math></u>	<u><math>\bar{M}_w/\bar{M}_n</math></u>	<u>Average Composition</u>	<u>Average Composition</u>		<u><math>\bar{K}_n</math></u>	<u><math>\bar{K}_w/\bar{K}_n</math></u>
					<u>0.1</u>	<u>0.5</u>		
0.1	0.1	31730	2.330	0.481	0.214	0.255	2.86	11.1
0.1	1.0	31730	2.390	0.481	0.195	0.229	2.86	10.1
0.1	10.0	31640	2.529	0.481	0.186	0.208	2.86	17.0
1.0	0.1	31240	1.903	0.480	0.347	0.421	2.88	1.89
1.0	1.0	31380	1.992	0.480	0.252	0.353	2.89	4.06
1.0	10.0	31710	2.211	0.481	0.195	0.244	2.89	13.4
10.0	0.1	31650	2.332	0.481	0.184	0.225	2.91	5.87
10.0	1.0	31650	2.440	0.481	0.184	0.211	2.92	12.0
10.0	10.0	31440	2.438	0.481	0.180	0.201	2.92	18.9

TABLE 6

Effect of Varying Degree of Polymerization ( $\bar{D}_p$ ) on the Influence of the Reaction Competitiveness Factor (RCF) and the Self-Affinity Factor (SAF) on the Molecular Weight, Hard Segment Length, and Composition Distributions

3/2/1 MDI/BD/PTMO-1000(H), NSA=10

$\bar{D}_p$	RCF	SA	$\bar{M}_n$	$\bar{M}_w/\bar{M}_n$	Fractional Composition		$\bar{K}_n$	$\bar{K}_w/\bar{K}_n$
					0.1	0.5		
10	0.1	0	3190	2.408	0.167	0.245	2.04	2.40
100	0.1	0	31730	2.309	0.223	0.266	2.86	11.6
300	0.1	0	92210	2.044	0.238	0.297	2.95	21.95
10	10	0	3173	2.362	0.1259	0.223	2.29	2.22
100	10	0	31650	2.281	0.192	0.282	2.91	2.96
300	10	0	90990	2.046	0.1940	0.286	2.97	5.01
10	1	1	3201	2.043	0.169	0.296	2.16	2.04
100	1	1	31380	1.992	0.252	0.353	2.89	4.06
300	1	1	90910	1.902	0.297	0.386	2.96	4.55

## Figure Captions

- Figure 1 Specific hard segment weight fraction versus cumulative weight fraction for the reference case with  $\bar{D}_p = 10, 100, \text{ and } 300$
- Figure 2a A three dimensional histogram of frequency of occurrence (z-axis versus molecular weight (y-axis) and hard segment weight fraction (x-axis) for the reference case with RCF = .1
- Figure 2b A three dimensional histogram of frequency of occurrence (z-axis versus molecular weight (y-axis) and hard segment weight fraction (x-axis) for the reference case with RCF = 1
- Figure 2c A three dimensional histogram of frequency of occurrence (z-axis versus molecular weight (y-axis) and hard segment weight fraction (x-axis) for the reference case with RCF = 10
- Figure 3 Specific hard segment weight fraction versus cumulative weight fraction for the reference case with RCF = .1, 1, and 10
- Figure 4a Hard segment length distribution (weight fraction) for the reference case with RCF = 1
- Figure 4b Hard segment length distribution (weight fraction) for the reference case with RCF = .1
- Figure 4c Hard segment length distribution (weight fraction) for the reference case with RCF = 10
- Figure 5 Specific hard segment weight fraction versus cumulative weight fraction for the reference case with SAF = 0, 1, and 10
- Figure 6a Three-dimensional histogram of the molecular weight, the weight fraction of hard segment, and the relative frequency of occurrence for the reference case with SAF = 1
- Figure 6b Three-dimensional histogram of the molecular weight, the weight fraction of hard segment, and the relative frequency of occurrence for the reference case with SAF = 10
- Figure 7 Specific hard segment weight fraction versus cumulative weight fraction for the reference case with RCF = .1 and SAF = 10

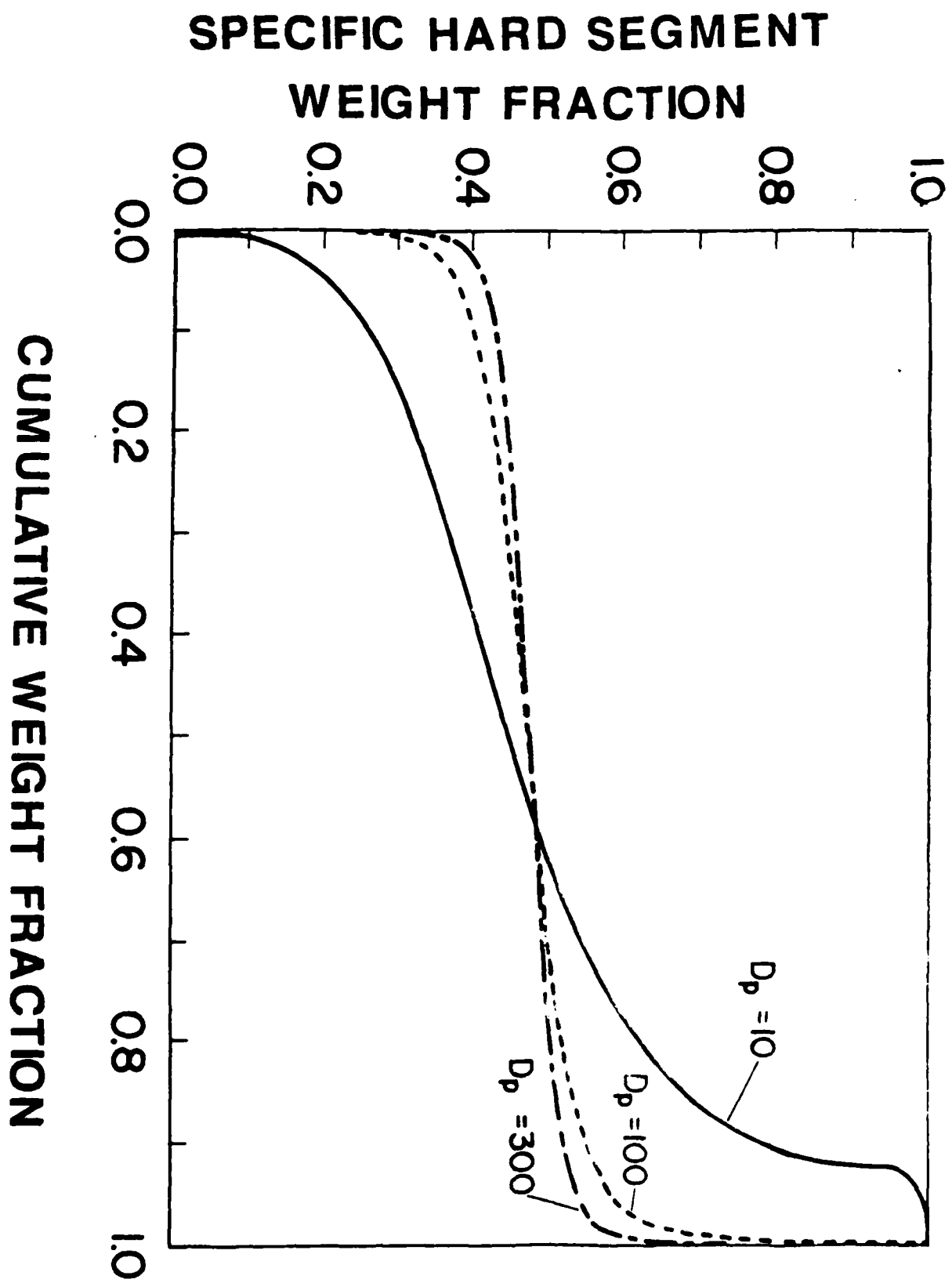


Figure 1

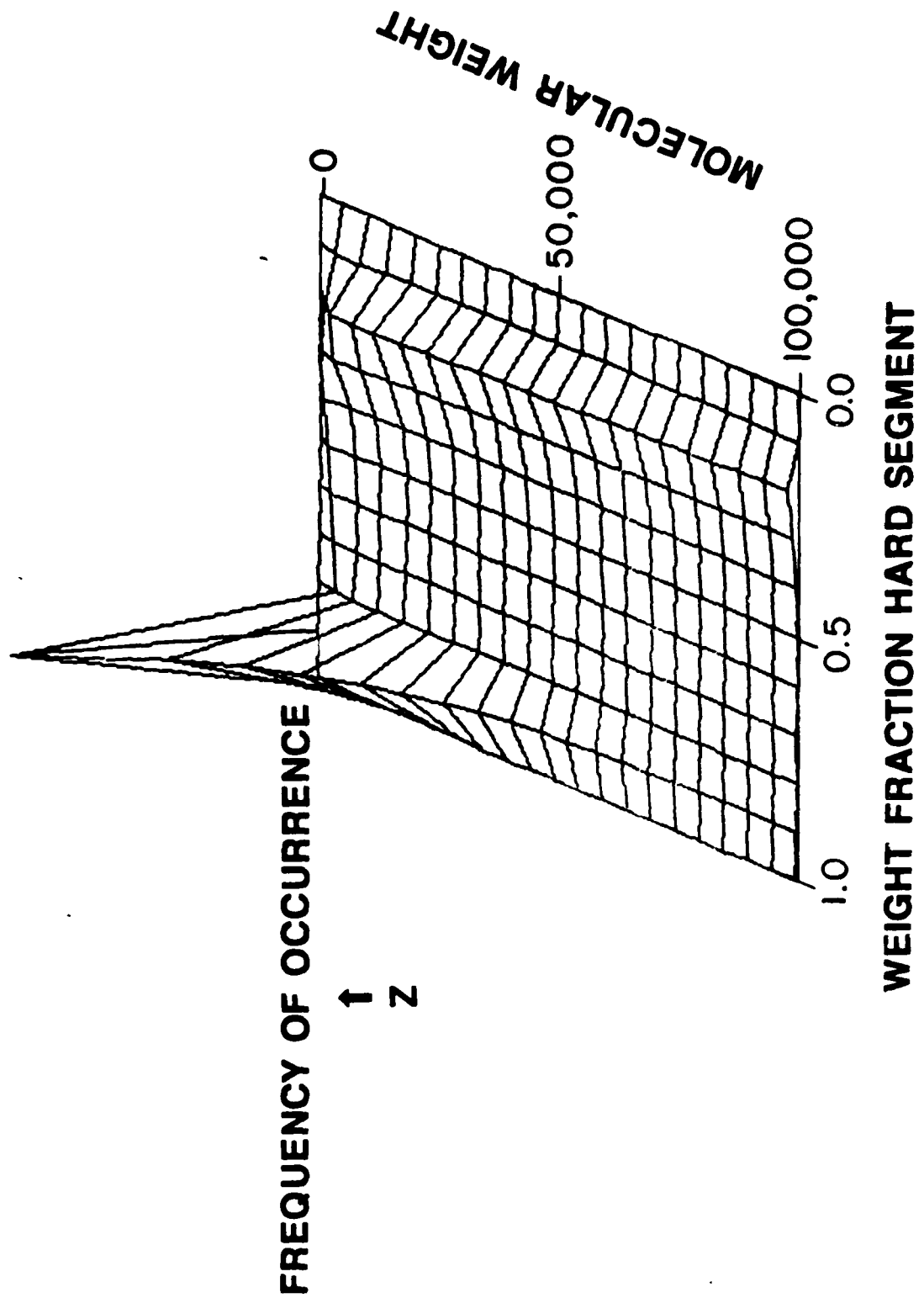


Fig. 2a

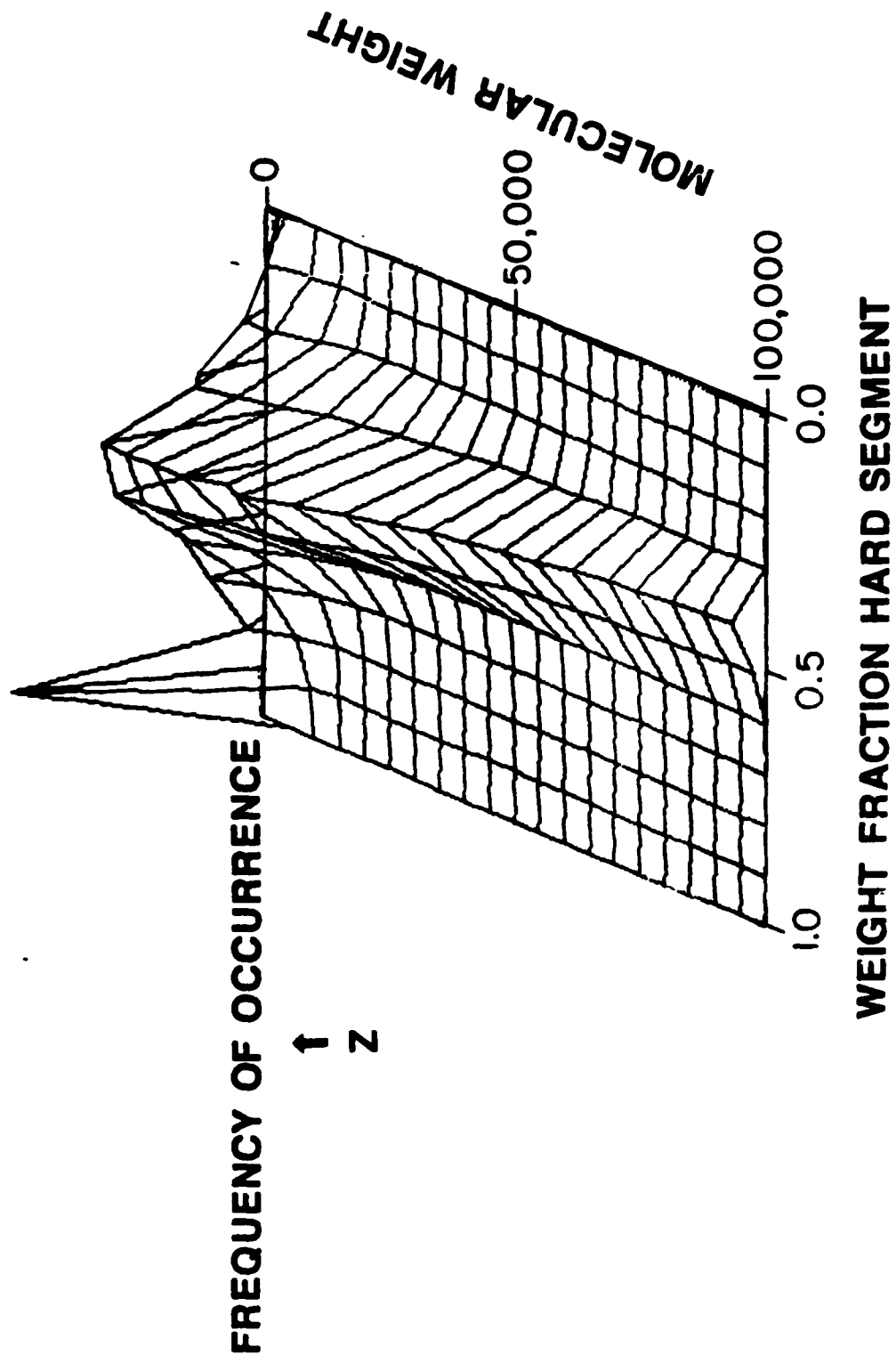


Fig. 2b

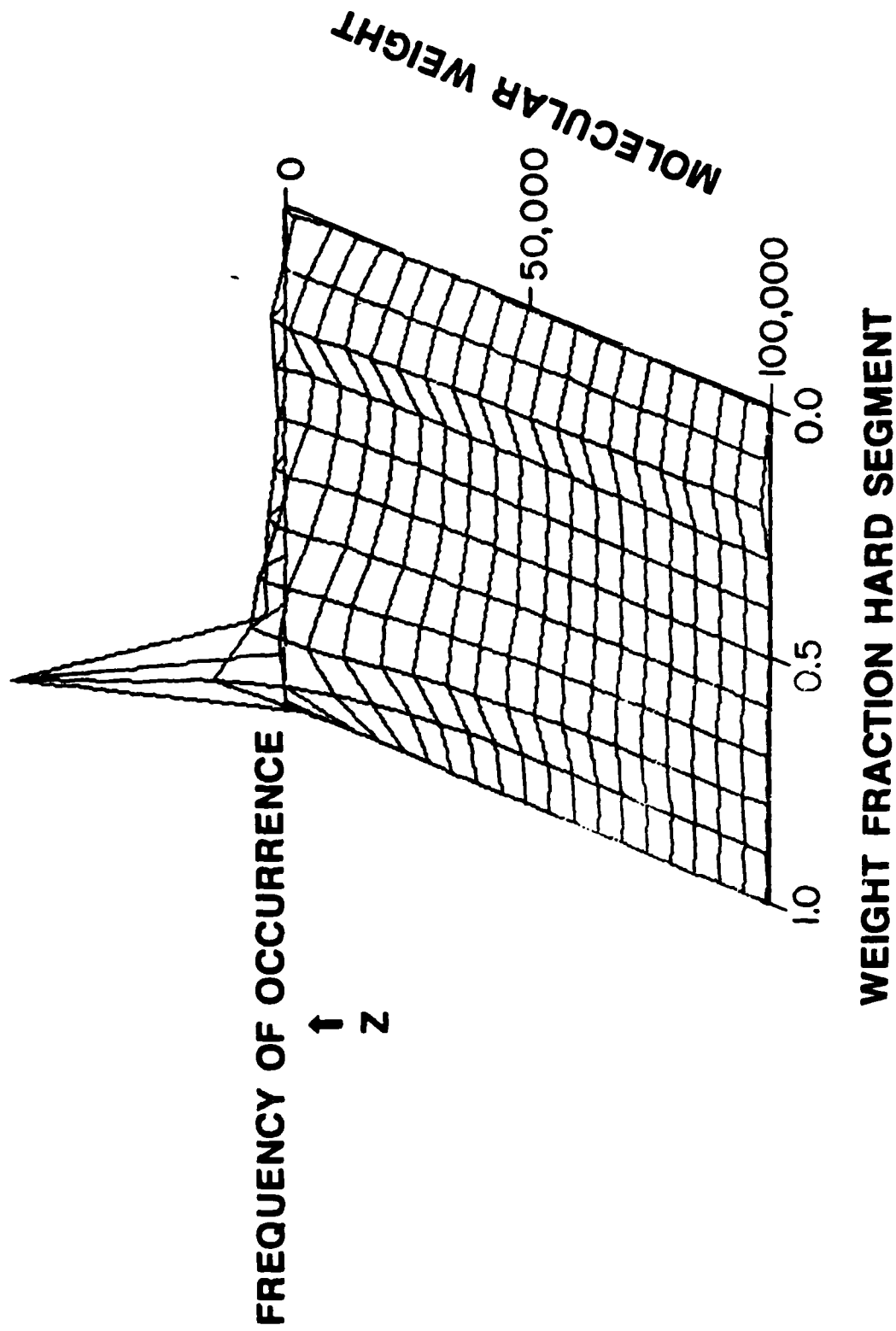


Fig. 2c

# SPECIFIC HARD SEGMENT WEIGHT FRACTION

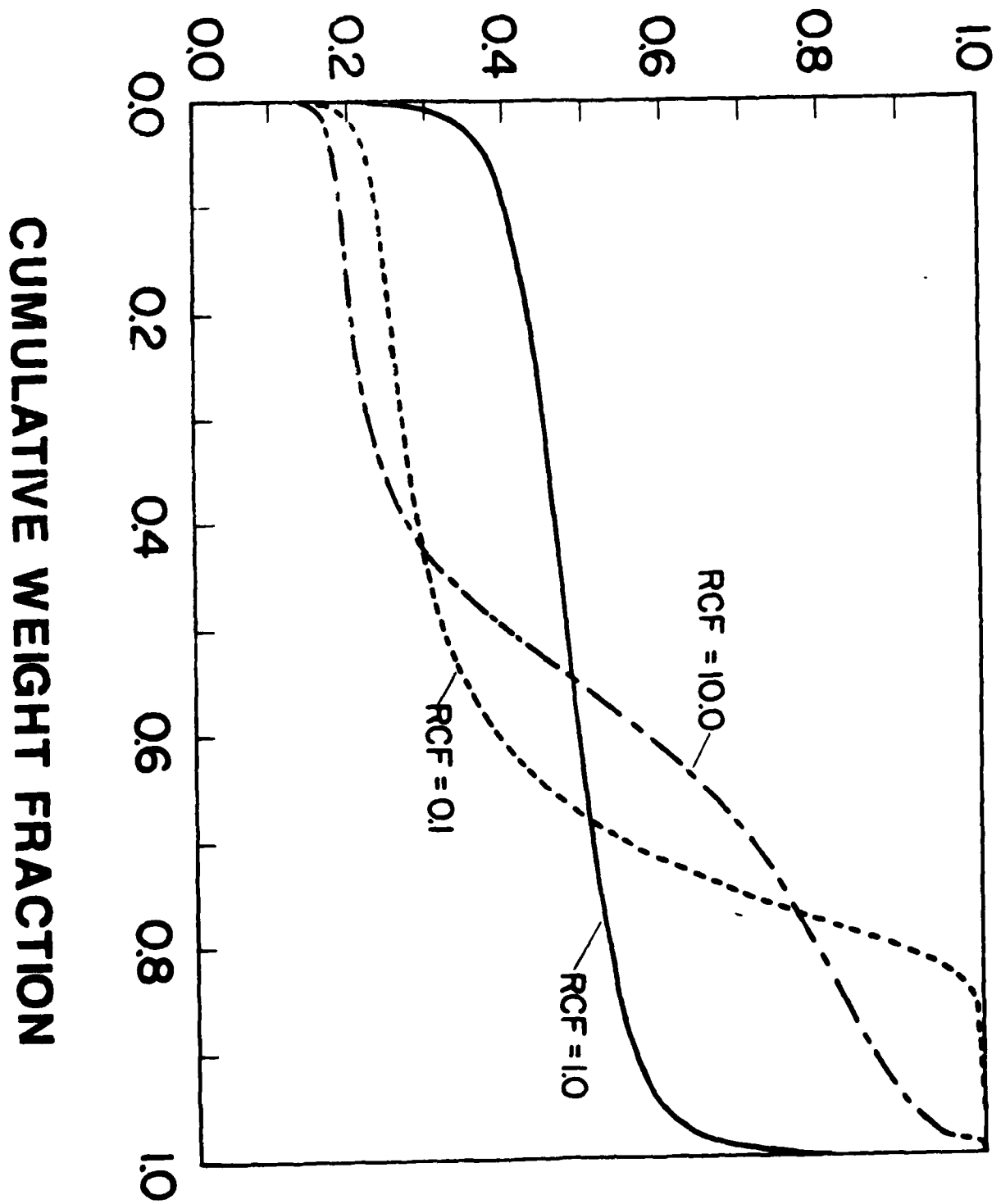
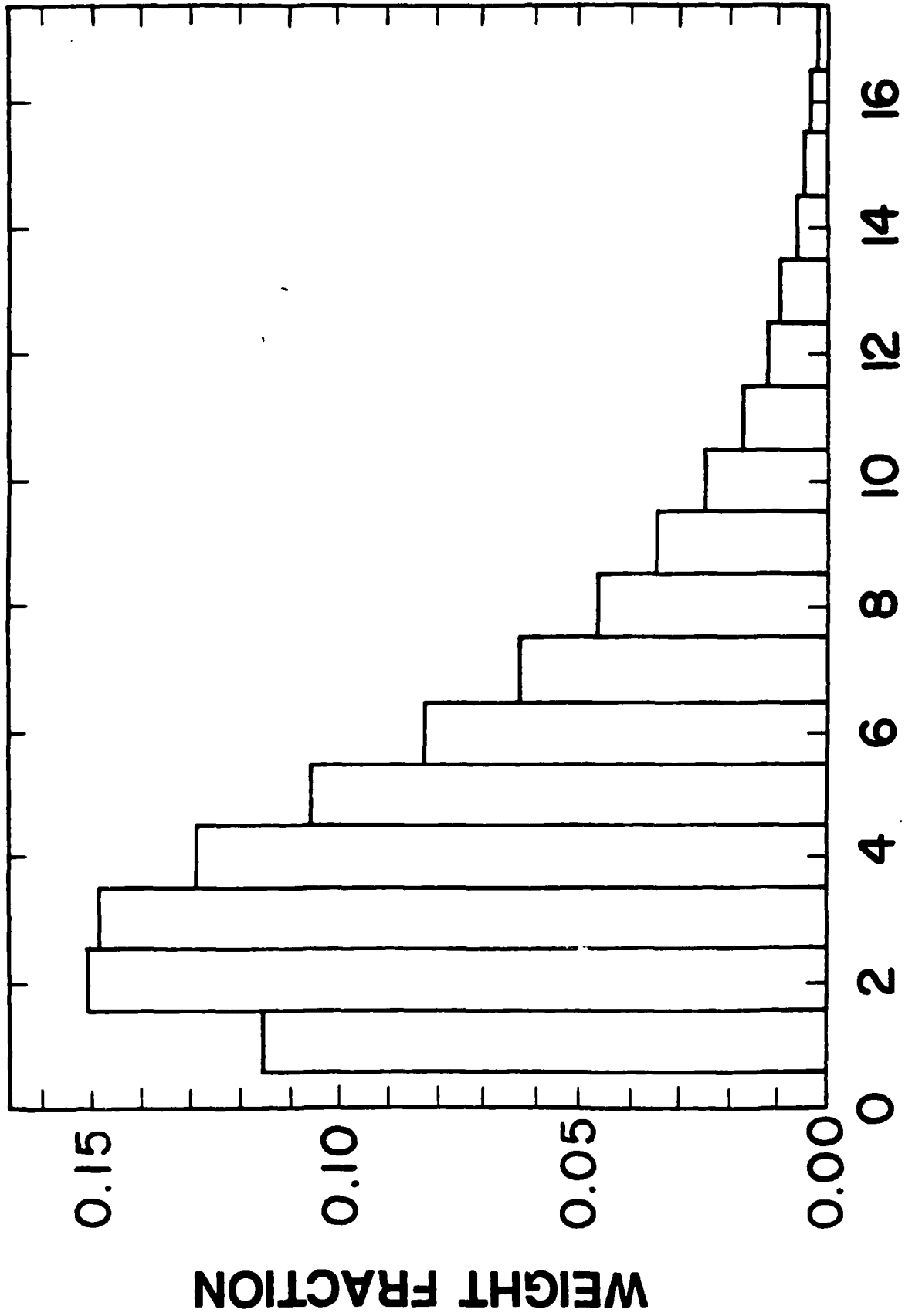


Fig. 3



NUMBER OF DIISOCYANATE UNITS

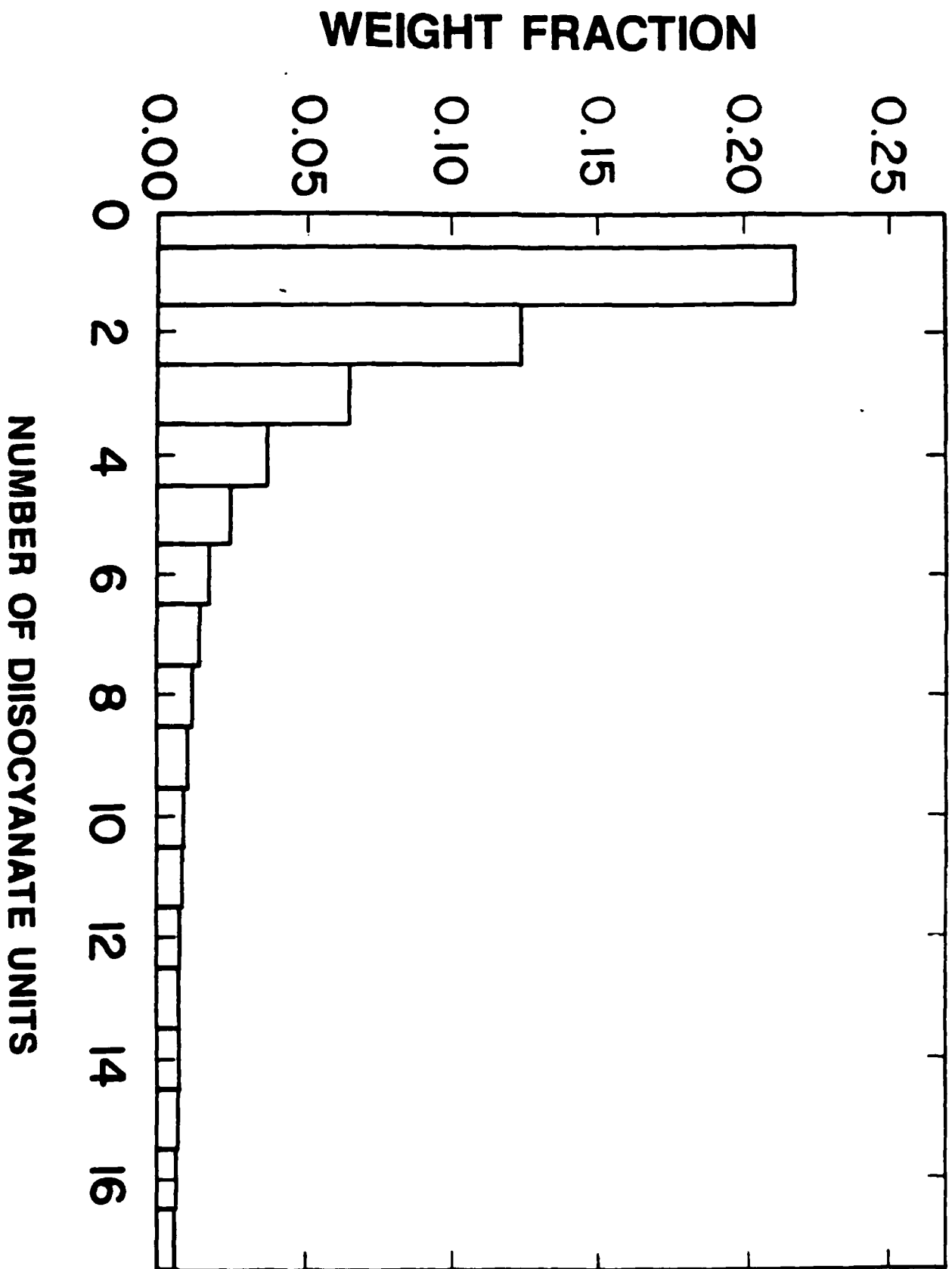
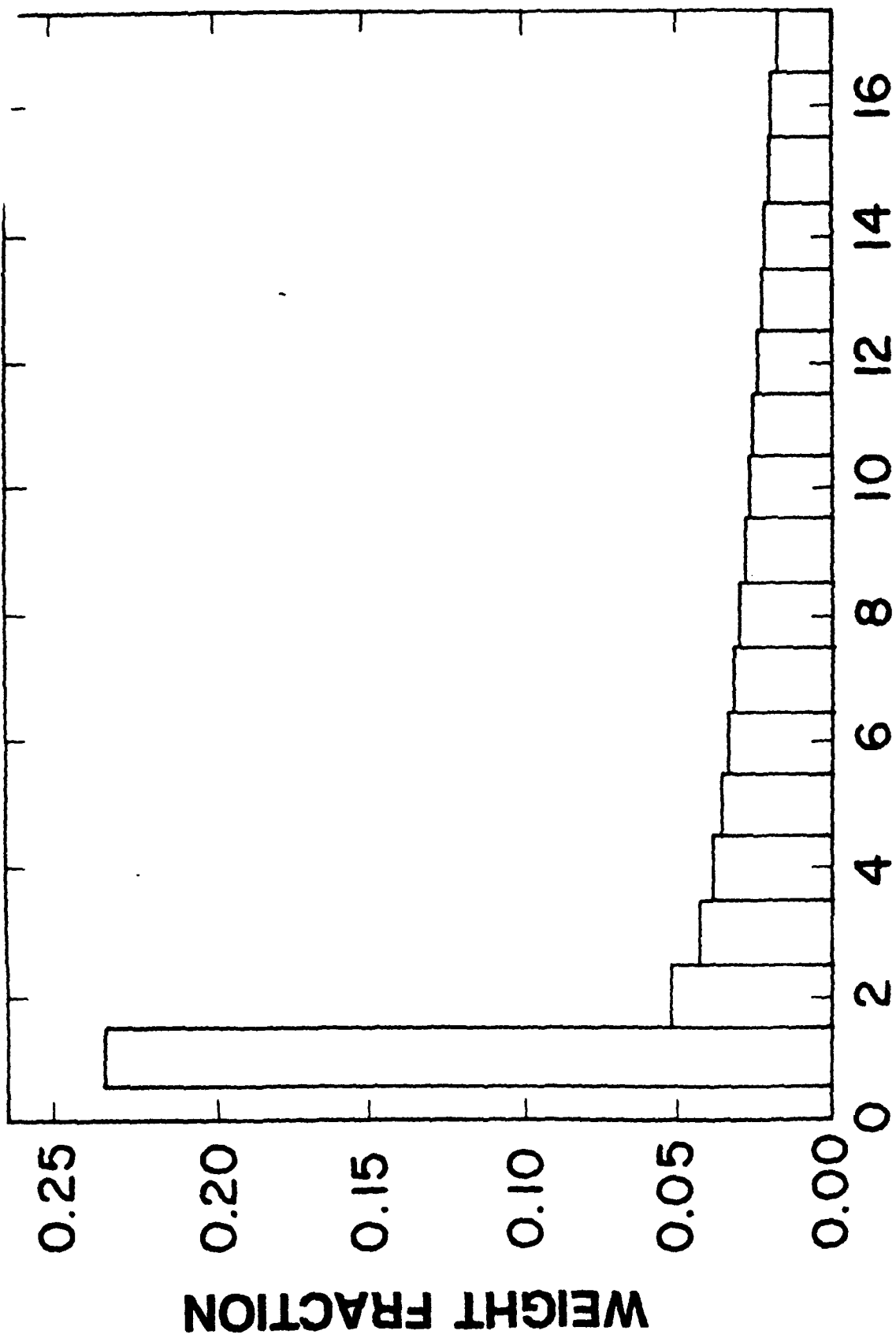


Fig 4b



**NUMBER OF DIISOCYANATE UNITS**

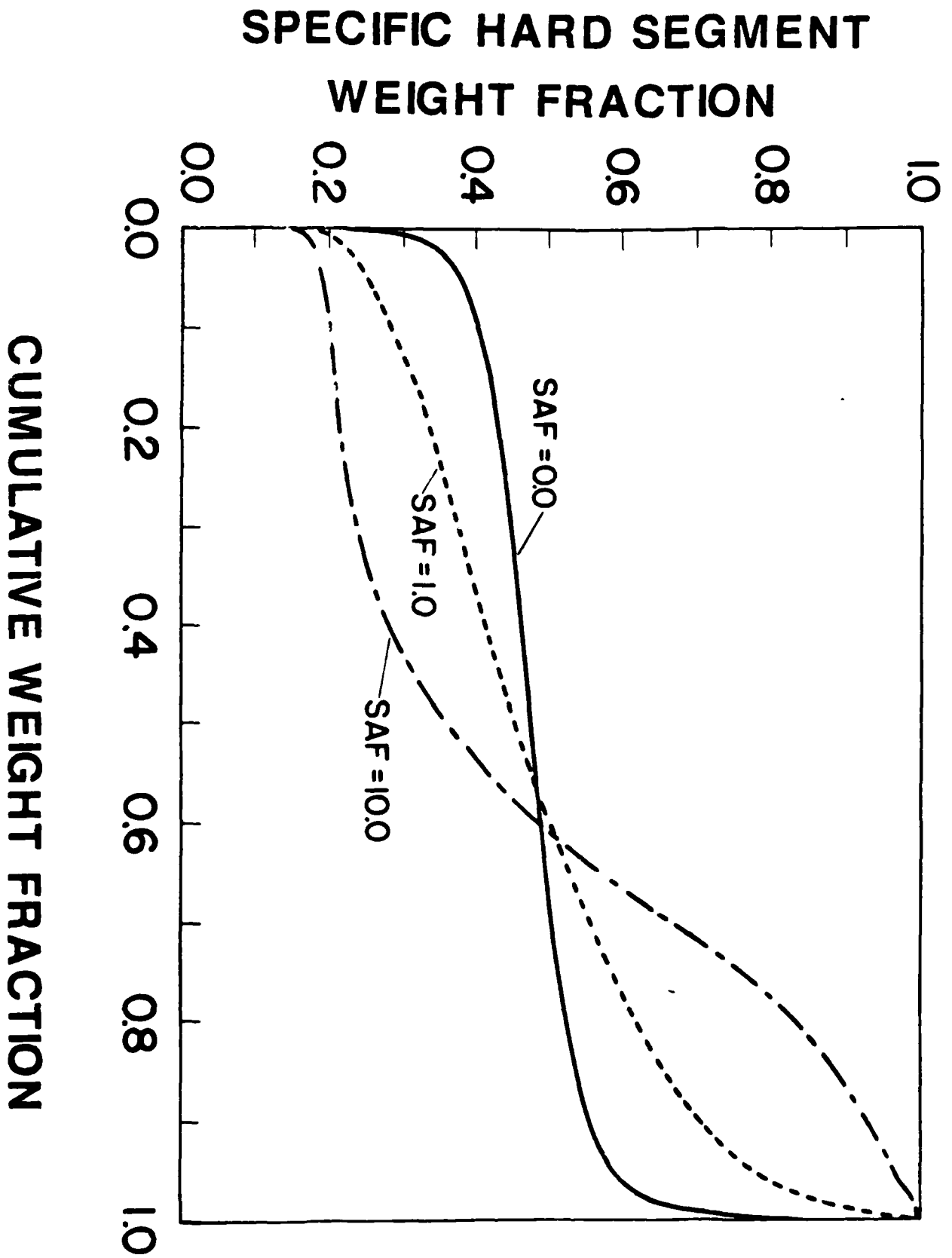


Fig. 5

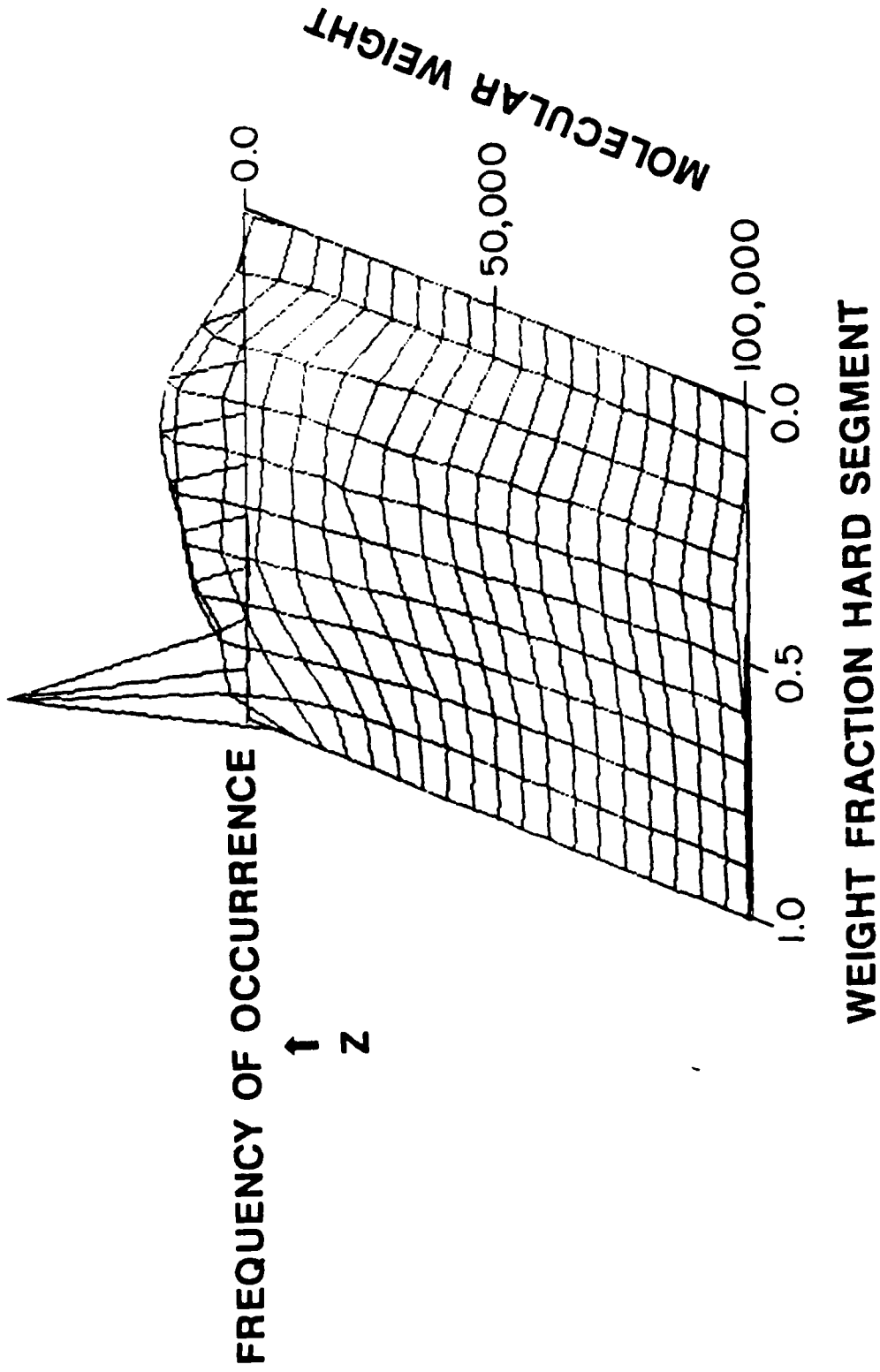


Fig. 6a

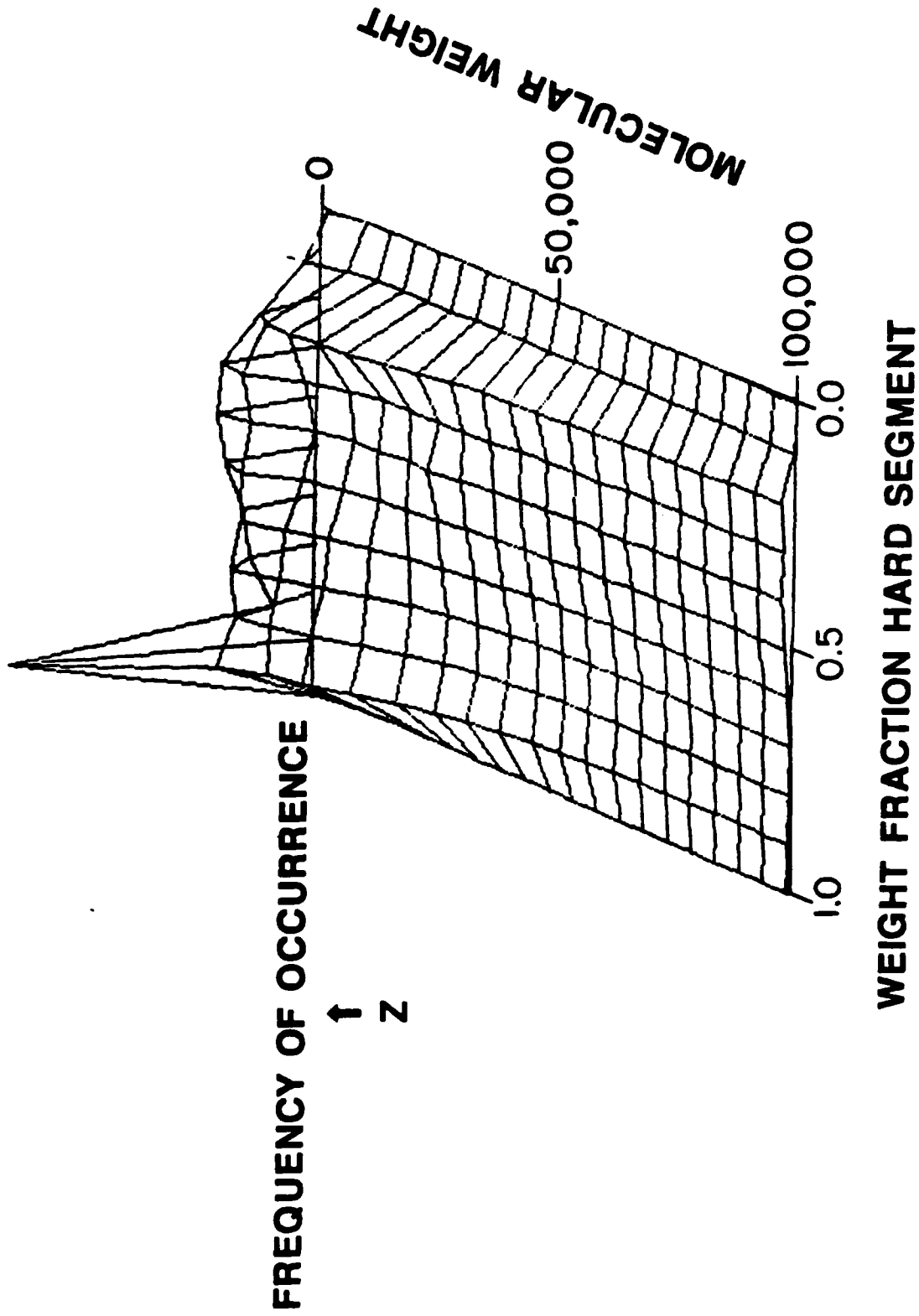


Fig. 6b

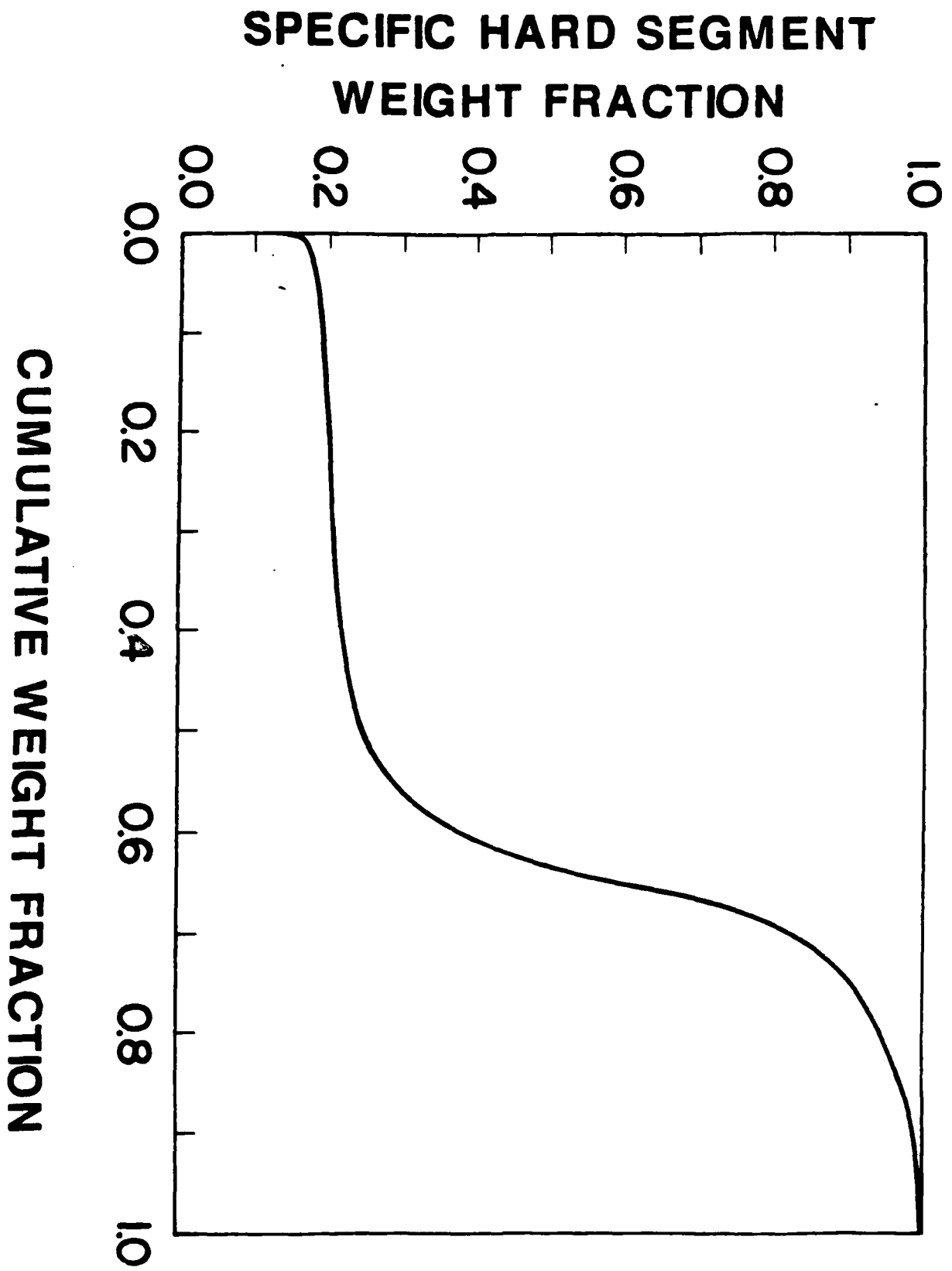


Figure 7

END

12-86

DTIC